

High quality NbTiN films fabrication and rapid thermal annealing investigation

Huan Ge(葛欢), Yi-Rong Jin(金贻荣), Xiao-Hui Song(宋小会)

Citation: Chin. Phys. B . 2019, 28(7): 077402. **doi:** 10.1088/1674-1056/28/7/077402
Journal homepage: http://cpb.iphy.ac.cn; http://iopscience.iop.org/cpb

What follows is a list of articles you may be interested in

Heat treatment on phase evolution of Bi-2223 precursor powder prepared by spray pyrolysis method

Li-Jun Cui(崔利军), Ping-Xiang Zhang(张平祥), Jin-Shan Li(李金山), Guo Yan(闫果), Yong Feng(冯勇), Xiang-Hong Liu(刘向宏), Jian-Feng Li(李建峰), Xi-Feng Pan(潘熙峰), Fan Yang(杨帆), Sheng-Nan Zhang(张胜楠), Xiao-Bo Ma(马晓波), Guo-Qing Liu(刘国庆)

Chin. Phys. B . 2019, 28(4): 047401. **doi:** 10.1088/1674-1056/28/4/047401

Synthesis, physical properties, and annealing investigation of new layered Bi-chalcogenide $LaOBiHgS_3$

Yi Yu(于一), Chunchang Wang(汪春昌), Liang Li(李亮), Qiuju Li(李秋菊), Chao Cheng(程超), Shuting Wang(王舒婷), Changjin Zhang(张昌锦)

Chin. Phys. B . 2019, 28(1): 017401. **doi:** 10.1088/1674-1056/28/1/017401

A single-crystal neutron diffraction study on magnetic structure of $CsCo_2Se_2$

Juanjuan Liu(刘娟娟), Jieming Sheng(盛洁明), Wei Luo(罗伟), Jinchen Wang(汪晋辰), Wei Bao(鲍威), Jinhu Yang(杨金虎), Minghu Fang(方明虎), S A Danilkin

Chin. Phys. B . 2018, 27(11): 117401. **doi:** 10.1088/1674-1056/27/11/117401

Tunneling field effect transistors based on in-plane and vertical layered phosphorus heterostructures

Shenyan Feng(冯申艳), Qiaoxuan Zhang(张巧璇), Jie Yang(杨洁), Ming Lei(雷鸣), Ruge Quhe(屈贺如歌)

Chin. Phys. B . 2017, 26(9): 097401. **doi:** 10.1088/1674-1056/26/9/097401

Critical current density behaviors across a grain boundary inclined to current with different angles in $YBa_2Cu_3O_{7-\delta}$ bicrystal junctions

Tao Hua(花涛), Wei-Wei Xu(许伟伟), Zheng-Ming Ji(吉争鸣), Da-Yuan Guo(郭大元), Qing-Yun Wang(王青云), Xiang-Rong Ma(马湘蓉), Rui-Yu Liang(梁瑞宇)

Chin. Phys. B . 2016, 25(6): 067401. **doi:** 10.1088/1674-1056/25/6/067401

High quality NbTiN films fabrication and rapid thermal annealing investigation*

Huan Ge(葛欢)[1], Yi-Rong Jin(金贻荣)[1,2], and Xiao-Hui Song(宋小会)[1,†]

[1] *Beijing National Laboratory for Condensed Matter Physics, Institute of Physics, University of Chinese Academy of Sciences, Beijing* 100190, *China*
[2] *Beijing Academy of Quantum Information Sciences, Beijing* 100193, *China*

(Received 28 January 2019; revised manuscript received 16 May 2019; published online 25 June 2019)

NbTiN thin films are good candidates for applications including single-photon detector, kinetic inductance detector, hot electron bolometer, and superconducting quantum computing circuits because of their favorable characteristics, such as good superconducting properties and easy fabrication. In this work, we systematically investigated the growth of high-quality NbTiN films with different thicknesses on Si substrates by reactive DC-magnetron sputtering method. After optimizing the growth conditions, such as the gas pressure, Ar/N_2 mixture ratio, and sputtering power, we obtained films with excellent superconducting properties. A high superconducting transition temperature of 15.5 K with narrow transition width of 0.03 K was obtained in a film of 300 nm thickness with surface roughness of less than 0.2 nm. In an ultra-thin film of 5 nm thick, we still obtained a transition temperature of 7.6 K. In addition, rapid thermal annealing (RTA) in atmosphere of nitrogen or nitrogen and hydrogen mixture was studied to improve the film quality. The results showed that T_c and crystal size of the NbTiN films were remarkably increased by RTA. For ultrathin films, the annealing in N_2/H_2 mixture had better effect than that in pure N_2. The T_c of 10 nm films improved from 9.6 K to 10.3 K after RTA in N_2/H_2 mixture at 450 °C.

Keywords: superconducting transition temperature, surface roughness, NbTiN film, rapid thermal annealing

PACS: 74.25.–q, 74.25.F–, 74.78.–w **DOI:** 10.1088/1674-1056/28/7/077402

1. Introduction

NbTiN thin films are widely investigated as candidates for many superconducting devices, including nanowire superconducting single photon detectors (SNSPD),[1–4] hot electron bolometer (HEB) mixers,[5–7] superconductor–insulator–superconductor (SIS) devices in the THz band,[8–10] and coplanar waveguide (CPW) superconducting resonators.[11] Unlike NbN films, the introduction of the third element can locally modify the atomic binding energy, leading to electronic structure and crystal lattice modifications.[12–14] Such modifications can improve the physical properties such as the electrical resistivity and the superconducting transition temperature.[14] In particular, it has been shown that NbTiN films surpass NbN films in many aspects for single-photon detectors because of the better uniformity and the smaller kinetic inductance.[15] In addition, NbTiN presents lower calculated surface impedance and better surface properties than NbN.

Several methods have been investigated to obtain high quality NbTiN thin films in the past few years. One of them is to introduce a buffer layer with the lattice constant similar to that of both the NbTiN film and the substrate. As a result, the lattice matching is improved and consequently the film quality is improved. For example, the AlN buffer layer can greatly improve the quality of NbTiN films.[16,17] This technique, although very effective, would introduce additional impurities, which thus degrades the device performance. Another method for high quality films is to grow the films on lattice-matched substrates. The NbTiN thin films fabricated on MgO or sapphire substrates usually have the high transition temperature and the low resistivity compared to those fabricated on Si or SiO_2/Si substrates.[18,19] In many applications, however, the silicon based substrates are preferred or even necessary for large-scale integrating due to the compatibility to semiconducting industry.

In the present study, we focused on the optimization of growth conditions for the NbTiN thin films on SiO_2/Si or intrinsic Si substrates. In addition, to further improve the superconducting properties of the NbTiN films, a rapid thermal annealing (RTA) method was also investigated at different temperatures. Post-annealing can promote the grain growth and decease the defects and disorders in the thin films, as discussed in Ref. [20]. However, some other previous results of annealing of Nb or NbN films showed degraded superconducting properties, possibly due to the oxygen atoms diffused into the grains.[21] Here, to clarify the annealing mechanism in nitride thin films, post-annealing of the NbTiN films was studied systematically. Our study shows that the transition temperature T_c increases evidently after RTA, but the residual resistivity increases too. As a comparison, we tried the thermal annealing treatment in both N_2 and N_2/H_2 mixture. The results show that T_c improvement is greater after annealing in N_2/H_2 mixture.

*Project supported by the Chinese Academy of Sciences Strategic Priority Research Program B (Grant No. XDB07010300) and the National Natural Science Foundation of China (Grant No. 11674376).

†Corresponding author. E-mail: xhsong@iphy.ac.cn

© 2019 Chinese Physical Society and IOP Publishing Ltd

2. Experiment

Our NbTiN thin films were deposited by reactive DC magnetron sputtering in a high vacuum chamber with base pressure down to 2.0×10^{-7} Pa. The target was an NbTi alloy with nominal compensation of 70% Nb and 30% Ti. The substrates were SiO_2/Si with 500 nm thick SiO_2 or Si(100) with high resistivity (> 10 kΩ·cm). Before sputtering, the substrates were pre-cleaned sequentially in acetone, ethanol, and distilled water by ultrasonic and then dried and degassed *in-situ* to over 100 °C for about 12–16 h. After some pre-sputtering to clean the target surface, the films were then deposited in an atmosphere of Ar/N_2 mixture of about 0.2–1 Pa with various powers. In addition, for investigating the influence of annealing, some films were annealed in N_2 atmosphere at 200–1000 °C with a rapid annealing furnace of Accu Thermo AW410, or in mixed atmosphere of 85% N_2 and 15% H_2 at 100–450 °C with a homemade annealing furnace.

The transport properties of the thin films were measured by the standard four-probe method in a Quantum DesignTM PPMS system. The lattice structural properties were determined by an x-ray diffractometer (XRD Ultima IV, Mac Science Co., Japan) and surface morphologies were observed by an atomic force microscope (American Asylum Research, MFP-3d-SA standard atomic force microscopy).

3. Results and discussion

The deposition parameters, such as the atmosphere pressure, Ar/N_2 mixture ratio, and sputtering power, can significantly influence the quality of the final films. To improve the superconducting transition temperature and surface smoothness, we systematically varied all these parameters in appropriate ranges and did transport, structural, and surface measurements for the corresponding films. Figures 1(a) and 1(b) show the T_c and surface roughness versus different sputtering pressures and powers, respectively. All these films were controlled with the thicknesses of about 300 nm.

When the sputtering pressure is low, the mean free path of the atoms increases and the averaged energy of the atoms enhances when hitting the substrates. As a result, the diffusion rate of atoms on top of the films increases, leading to a smooth surface morphology. However, if the pressure is lowered, the stress in the films increases, leading to the increasing of defects and thus the drop of T_c. If the pressure is increased, the surface roughness increases too. This is because the deposited atoms do not have enough energy to move to the proper positions, as a result, form a rough surface. A smooth surface is particular important for some applications, for example, the fabrication of superconducting microelectronic devices such as SIS junction. Kohlstedt *et al.*[22] showed that the roughness of the film surface strongly influences the tunnel barrier formation and the electrical properties of the barrier. With the optimal sputtering pressure, fairly smooth surfaces with 0.15 nm roughness were obtained for our 300 nm films.

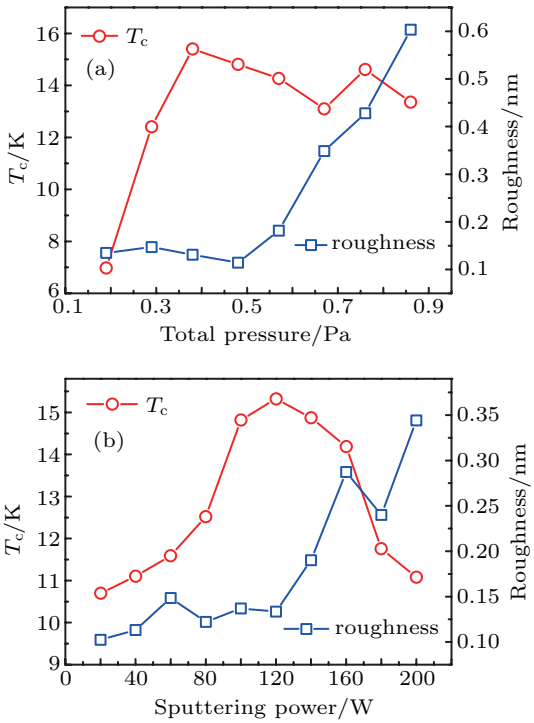


Fig. 1. The dependence of superconducting transition temperature T_c and surface roughness on (a) the total Ar and N_2 gas pressure and (b) the sputtering power during magnetron sputtering (film thickness 300 nm).

High sputtering power leads to high growth rate of the films, which avoids the impurity gas contamination, especially for active elements like Nb, Ti, and so on. As a result, increasing the sputtering power to an appropriate level usually improves the film quality. However, with the further increase of the growth rate, atoms will not have enough time to move to low energy positions before they are buried by newly arrived atoms. This will generate more defects in the films, thus decrease T_c and increase the surface roughness. Our data show this phenomenon (Fig. 1(b)).

Figure 2(a) shows some typical ρ–T curves for different thickness NbTiN films fabricated with optimized sputtering conditions (the sputtering power was decreased to 40 W for the ultrathin films when the thicknesses were lower than 30 nm). The superconducting transition temperature T_c and transition width ΔT_c (the temperature interval of 90%$\rho_{20\ K}$ to 10%$\rho_{20\ K}$) as the function of thickness from 5 nm to 300 nm are shown in Fig. 2(b). Consistent with the behavior of the Nb films,[23] T_c increased with the film thickness and was 14.2 K for 100 nm thickness films. A maximum T_c of 15.5 K was obtained for 300 nm thickness films. The T_c was 7.6 K for the thinnest 5 nm films and 9.6 K for the 10 nm films; to our knowledge these are fairly good results for ultrathin NbTiN films grown on Si substrates at room temperature without buffer layer to decrease the lattice mismatch. The superconducting transition

widths of our NbTiN films were quite narrow, about 0.07 K for 100 nm films and 0.03 K for 300 nm films, which indicates the exceeding uniform of our NbTiN films. Figure 3 shows the AFM images for films with different thicknesses (under the same deposition conditions). From the surface morphology we could not identify clearly the grains until the thickness increased to 300 nm (with grain size about 14 nm). Such surface topography indicates the amorphous growth characteristics because of the ternary elements constitute of the NbTiN films. The ultralow surface roughnesses, 0.1 nm for 10 nm film and 0.18 nm for 300 nm films, also show the amorphous growth mechanism of the NbTiN films.

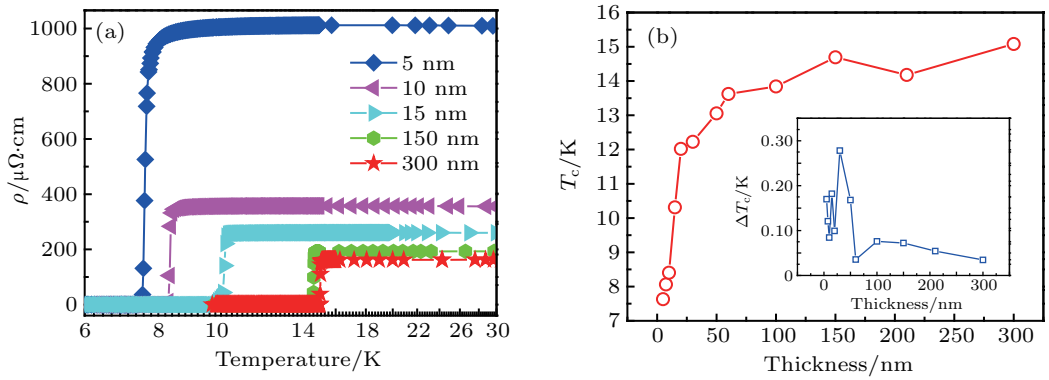


Fig. 2. (a) Some representative resistivity versus temperature for different thickness NbTiN films. (b) Superconductor transition temperature T_c and superconductor transition width ΔT_c (from $90\%\rho_{20\,K}$ to $10\%\rho_{20\,K}$) (inset) for different thickness films.

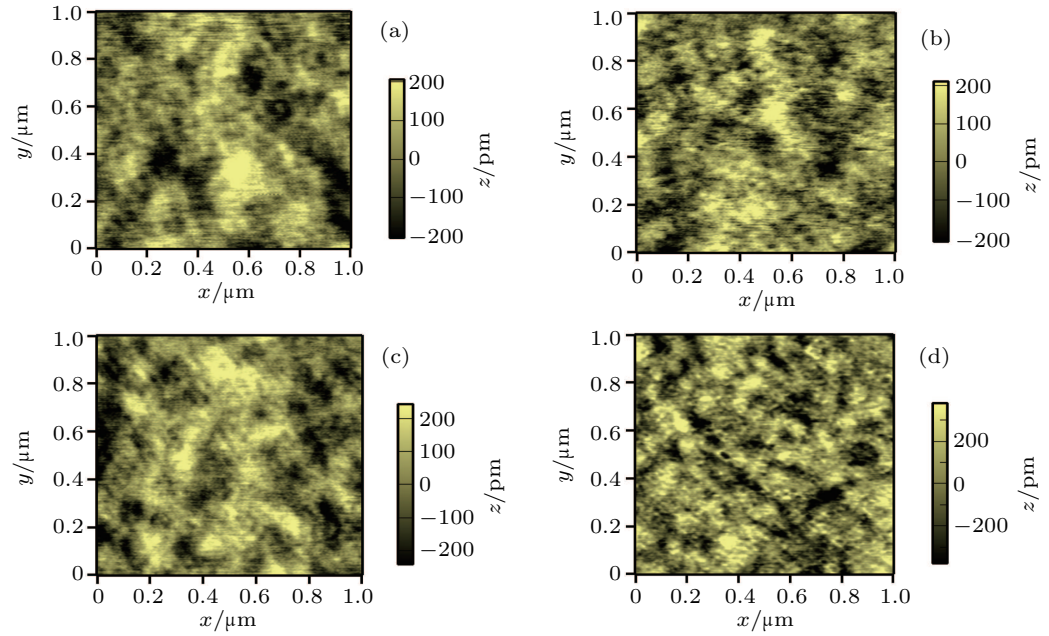


Fig. 3. The AFM topographic images of NbTiN thin films with thicknesses of (a) 10 nm, (b) 30 nm, (c) 60 nm, and (d) 300 nm.

To study the effect of thermal treatment on NbTiN thin films, the NbTiN films of different thickness (10–300 nm) were annealed by rapid thermal annealing (RTA) method with temperature ranging from 200 °C to 1000 °C. The annealing atmosphere was chosen as N_2 or N_2/H_2 mixture (85% of N_2 and 15% of H_2) for comparison. In pure N_2, the films were rapidly heated to the settled temperature within 30 s, and held at that temperature for 10 min, then decreased to 40 °C within 3 min. In N_2/H_2 mixture, the temperature increased to the annealing temperature within 180 s, held for 10 min, and then naturally cooled down to room temperature. Figure 4(a) shows the x-ray diffraction (XRD) results for the 300 nm films before and after RTA in N_2 atmosphere. The [111] and [200] diffraction peaks were both present for the as-deposited and annealed films. Increasing the annealing temperature resulted in an increase in the ratio of the [200] and [111] x-ray diffraction line intensities (see Fig. 4(b)). These results indicate that as the annealing temperature increased, a change in texture from [111] to [100] took place, which supports Iosad *et al.* argument[24] that the thermalization of films during annealing causes the increase of the atomic energy, resulting in the preferred growth of [100] direction. The inset of Fig. 4(b) shows the proportional growth of grain size in [200] direction with increasing annealing temperature. The grain size increased from 14.5 nm

for the as-deposited films to 22.7 nm after RTA at 1000 °C.

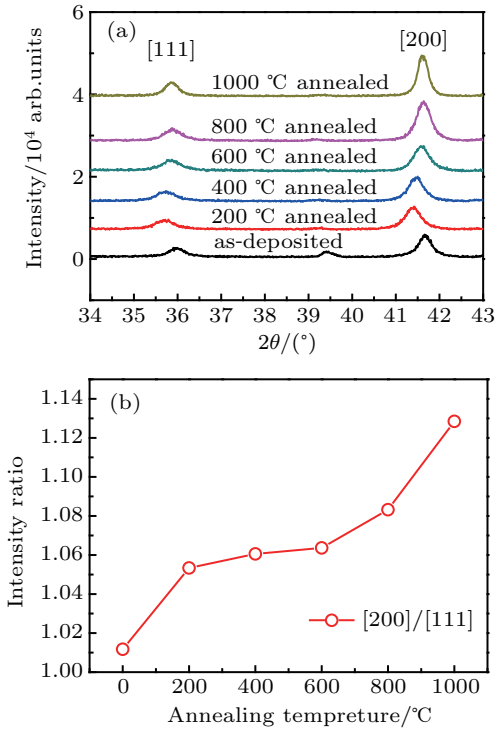


Fig. 4. (a) XRD patterns of 300 nm NbTiN films rapid thermal annealing in N_2 atmosphere. (b) The ratio of [200] and [111] XRD peaks as the function of annealing temperature. The inset shows the grain size increasing with the RTA temperature.

Figure 5 shows the resistivity versus temperature curves of 100 nm films and the change percentage of T_c for different thickness films before and after RTA in N_2 atmosphere. The T_c of the 100 nm films increased from 14.2 K to 14.8 K after 1000 °C thermal annealing . The improvement of T_c was more obviously for the relative thinner films, such as 30 nm and 60 nm films. After 1000 °C RTA, T_c increased about 12% for 30 nm, 60 nm thin films (11.3 K to 12.7 K for 30 nm films, 12.0 K to 13.5 K for 60 nm films), only 4.5% for 100 nm films. Along with the increase of T_c after thermal annealing, we found that the residual resistivity of the films increased with the increase of the RTA temperature. Such behavior contradicts with the thermal annealing effect of normal metals, where post-annealing increases the grain size and decreases the grain boundary scattering, as a result, leads to the decrease of the resistivity. We believe that this phenomenon may connect with the transport mechanism in nitride films. Chockalingam *et al.* proposed[25] that the T_c of NbN films is governed primarily by the carrier density rather than the disorder scattering. The Hall effects were measured for both as-deposited and 1000 °C RTA in N_2 atmosphere 300 nm NbTiN films. The results showed that the carrier density decreased after RTA, from 1.74×10^{28} e/m^3 for the as-deposited film to 1.34×10^{28} e/m^3 for the 1000 °C annealed one. These results offered a reasonable explanation for the increase of the resistivity after RTA. However, these results could not give hints for T_c enhancement of NbTiN films after RTA. The increase of grain sizes after RTA may be the reason for the improvement of superconductivity properties. The discussion in Refs. [23] and [25] showed that the factor influencing the superconductivity transition temperature was complex for Nb or NbN films. For three-element superconductivity material NbTiN films, the intrinsic mechanism of superconductivity may be more complex, which needs further investigation for more details.

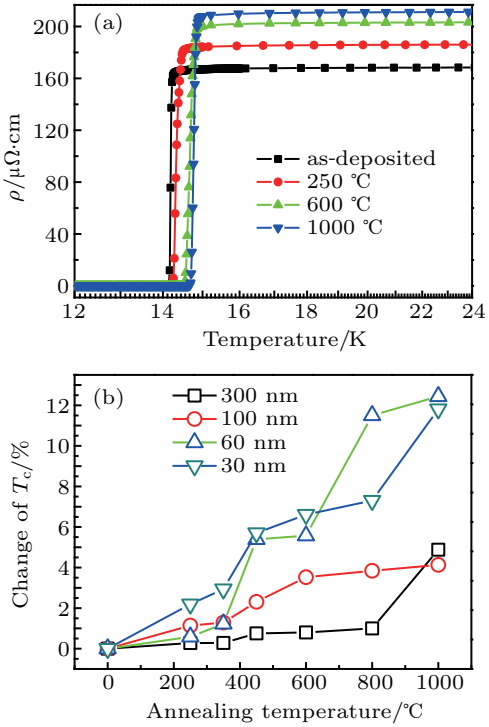


Fig. 5. (a) The resistivity versus temperature curves of 100 nm films before and after RTA. (b) The variation percent of T_c before and after RTA in N_2 atmosphere for different thickness films.

For the thinner films of 10 nm, the situation changed. We found that T_c decreased after annealing at 450 °C in N_2 atmosphere. When we changed the atmosphere to N_2/H_2 mixture, however, T_c kept increasing. These results are shown in Fig. 6(a). Furthermore, as a comparison, we annealed films of different thicknesses in these two kinds of atmospheres, and the results are shown in Fig. 6(b). It can be seen that T_c after RTA in N_2/H_2 mixture is generally higher than that in N_2. As we know, the main difference of pure N_2 and N_2/H_2 mixture is the introduction of deoxidizing hydrogen gas. Post-annealing in N_2 atmosphere avoids the further oxidation and decreases the nitrogen defect in nitride films. However, there is usually a natural oxidized layer on the film surface after it is taken out from the sputtering chamber. Zhang *et al.*[26] showed that there is an about 1.3 nm thick oxidized layer of Nb_2O_5, TiO_2, and NbO on top of NbTiN films. We believe that the high temperature thermal treatment induces the surface oxygen atoms diffusion into the grain boundary, as a result leads to the decrease of T_c even if the annealing is carried out in N_2 atmosphere. While the films are treated in a reducing atmosphere,

in our case, N_2/H_2 mixture, hydrogen atoms can take the oxygen atoms from the surface and prevent them diffuse into the films, resulting in T_c improvement. The ultrathin films were more sensitive to the influence of the surface oxidized layer because of the high ratio of the surface layer. The T_c of 10 nm ultrathin films increased from 9.6 K to 10.3 K after RTA in N_2/H_2 at 450 °C. These results can help us further understand the surface properties of ultrathin NbTiN films for improving the performance of NbTiN-based devices.

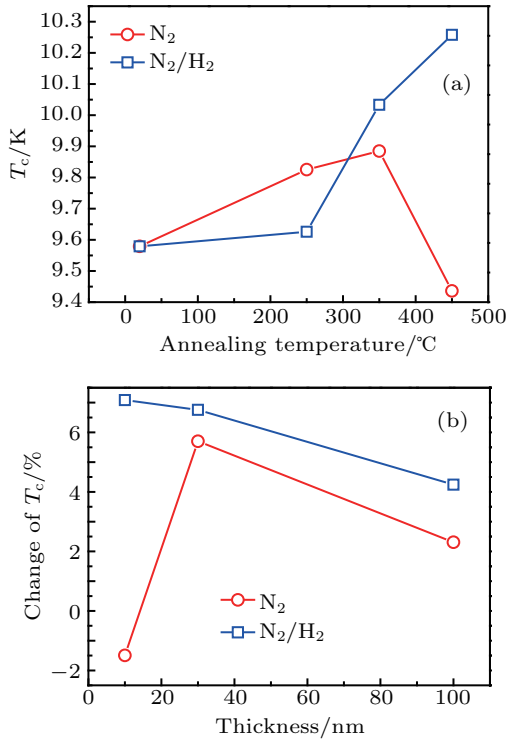


Fig. 6. (a) The relationship between superconductor transition temperature and annealing temperature for 10 nm NbTiN films in N_2 or N_2/H_2 mixture. (b) The rise of T_c after RTA at 450 °C in two kinds of atmospheres.

4. Conclusion

High quality NbTiN films with high transition temperature, narrow transition width, and smooth surfaces were fabricated by optimizing the sputtering conditions including the pressure, N_2/Ar mixture ratio, and sputtering power. We obtained T_c as high as 15.5 K and ΔT_c as low as 0.03 K in a 300 nm NbTiN film on SiO_2/Si substrate. We also obtained T_c of 7.6 K in a 5 nm film on intrinsic Si substrate without extra treatment and the growth of a buffer layer. Rapid thermal annealing after film deposition was carried out in N_2 or N_2/H_2 mixture atmosphere. X-ray diffraction results showed that the grain size increased with the increase of the annealing temperature, and the film texture generally changed from [111] to [100] facet. The T_c increased evidently after RTA, but the residual resistivity also increased. As a comparison, we tried the thermal annealing treatment in both N_2 and N_2/H_2 mixed atmospheres. The results showed that T_c improvement is higher after the treatment in N_2/H_2 mixture.

References

[1] Tanner M G, Natarajan C M, Pottapenjara V K, O'Connor J A, Warburton R J, Hadfield R H, Baek B, Nam S, Dorenbos S N, Bermudez Urena E, Zijlstra T, Klapwijk T M and Zwiller V 2010 *Appl. Phys. Lett.* **96** 221109
[2] Schuck C, Pernice W H P and Tang H X 2013 *Sci. Rep.* **3** 1893
[3] Zadeh I E, Johannes W N Los, Gourgues R B M, Steinmetz V, Dobrovolskiy S M, Zwiller V and Dorenbos S N 2017 *APL Photon.* **2** 111301
[4] Jia X Q, Kang L, Yang X Z, Wang Z H, Ren T K, Jin B B, Chen J, Xu W W and Wu P H 2015 *IEEE Trans. Appl. Supercond.* **25** 3
[5] Jiang L, Shiba S, Shimbo K, Sakai N, Yamakura T, Sugimura M, Ananthasubramanian P G, Maezawa H, Irimajiri Y and Yamamoto S 2009 *IEEE Trans. Appl. Supercond.* **19** 3
[6] Jiang L, Shiba S, Shiino T, Shimbo K, Sakai N, Yamakura T, Irimajiri Y, Ananthasubramanian P G, Maezawa H and Yamamoto S 2010 *Supercond. Sci. Technol.* **23** 4
[7] Shiba S, Irimajiri Y, Yamakura T, Maezawa H, Sekine N, Hosako I and Yamamoto S 2012 *IEEE Trans. Appl. Supercond.* **2** 1
[8] Westig M P, Selig S, Jacobs K, Klapwijk T M and Honingh C E 2013 *J. Appl. Phys.* **114** 124504
[9] Jackson B D, Baryshev A M, Lange G de, Gao J R, Shitov S V, Iosad N N and Klapwijk T M 2001 *Appl. Phys. Lett.* **79** 436
[10] Akaike H, Sakamoto S, Munemoto K and Fujimaki A 2016 *IEEE Trans. Appl. Supercond.* **26** 5
[11] Bruno A, Lange G de, Asaad S, Enden K L van der, Langford N K and DiCarlo L 2015 *Appl. Phys. Lett.* **106** 182601
[12] Myoren H, Shimizu H, Iizuka T and Takada S 2001 *IEEE. Trans. Appl. Supercond.* **11** 3828
[13] Yu L, Singh R K, Liu H, Wu S Y, Hu R, Durand D, Bulman J, Rowell J M and Newman N 2005 *IEEE Trans. Appl. Supercond.* **15** 44
[14] Makise K, Terai H, Takeda M, Uzawa Y and Wang Z 2011 *IEEE Trans. Appl. Supercond.* **21** 139
[15] Yang X Y, You L X, Zhang L, Lv C L, Li H, Liu X Y, Zhou H and Zhen Wang 2018 *IEEE Trans. Appl. Supercond.* **28** 1
[16] Shiino T, Shiba S, Sakai N, Yamakura T, Jiang L, Uzawa Y, Maezawa H and Yamamoto S 2010 *Supercond. Sci. Technol.* **23** 045004
[17] Loudkov D, Tong C Y E, Blundell R, Megerian K G and Stern J A 2005 *IEEE Trans. Appl. Supercond.* **15** 476
[18] Zhang L, Peng W, You L X and Wang Z 2015 *Appl. Phys. Lett.* **107** 122603
[19] Guziewicz M, Laszcz A, Domagala J Z, Golaszewska K, Ratajczak J, Kruszka R, Juchniewicz M, Czerwinski A and Slysz W 2013 *Proc. SPIE* **8902** 89022S
[20] Zhang X, Song X H and Zhang D L 2010 *Chin. Phys. B* **19** 086802
[21] Hatano M, Nishino T and Kawabe U 1988 *J. Vac. Sci. Technol.* **6** 2381
[22] Kohlstedt H, Konig F, Henne P, Thyssen N and Caputob P 1996 *J. Appl. Phys.* **80** 9
[23] Song X H, Jin Y R, Fan Z J, Mi Z Y and Zhang D L 2015 *Chin. Phys. Lett.* **32** 047403
[24] Iosad N N, Pers N M van der, Grachev S, Roddatis V V, Jackson B D, Polyakov S N, Dmitriev P N and Klapwijk T M 2002 *J. Appl. Phys.* **92** 9
[25] Chockalingam S P, Chand M, Jesudasan J, Tripathi V and Raychaudhuri P 2008 *Phys. Rev. B* **77** 214503
[26] Zhang L, You L X, Ying L L, Peng W and Wang Z 2018 *Physica C* **545** 1